ORIGINAL ARTICLE

Deepening the synergistic role of additive manufacturing and computational strategies in jewellery

Noemi Cerrato[1] · Elisabetta Gariboldi[2] · Michela Ferraro[3] · Sara Candidori[2] · Serena Graziosi[2]

Abstract

This study investigates the synergy between additive manufacturing (AM) technologies and computational design strategies in jewellery and how that synergy can be successfully exploited to extend innovation in that field further. A case study called Ecdysis, a bioinspired jewellery collection, is presented. A dedicated computational algorithm has been developed and is described in detail. This algorithm allows for the exploitation of the shape and functional complexity dimensions allowed by AM and the control of the printability of the generated concept. Shape and functional complexity are exploited to mimic the beauty and dynamism of snakes' slithering mechanism. At the same time, starting from the developed algorithm, multiple digital models and physical prototypes have been fabricated, leveraging material extrusion, vat photopolymerisation, and powder bed fusion processes. This further development step of the collection thus confirms the versatility of both the proposed approach and AM technologies for jewellery. Therefore, the paper demonstrates how unique wearing experiences can be created and how uniqueness can be simultaneously preserved and democratised in jewellery by deepening the synergy between AM technologies and computational strategies.

Keywords Design for additive manufacturing · Jewellery · Interaction design · Computational design · Bioinspired design

1 Introduction

Additive manufacturing (AM) processes have opened new design scenarios regarding shape, material, and functional complexity [1]. Shape complexity can now be reached at multiple scales [1]. Material complexity concerns the possibility of tuning material properties locally [1]. Functional complexity concerns the possibility of printing working mechanisms and embedding external components inside [1]. All these design dimensions and other opportunities are summarised within the *Design for Additive Manufacturing (DfAM)* topic [1]. This increased design freedom and complexity has further stimulated the possibility of mimicking and/or implementing natural principles and structures into physical objects in multiple fields [2]. For example, in the field of wearables, pioneering products developed exploiting 3D printing, computation, and bioinspiration, among others, are the *Hyphae* [3] and *Florescence* [4] jewellery collections, designed by the generative design studio Nervous System [5]. *Hyphae* jewels are inspired by the structure of the veins of organisms [3]. *Florescence* exploits the growing process of flowers and of the arms of jellyfish [4]. Another visionary project is *Mushtari* [6], part of the *Wanderers* collection [7]. It is a fluidic wearable designed to act as a potential environment for the culture of microorganisms to impart biological functionalities [6].

These cases confirm that the binomial between digitalisation, including AM technologies and computational strategies, and nature has already been successfully explored. Together with these iconic examples, other studies have also discussed and, in some cases, applied computational strategies in jewellery to support generative design and customisation [8–10]. The approaches available are multiple and focused on supporting the generation of shapes by exploiting optimisation [9], math-inspired approaches and forms [8, 9, 11], and strategies for topological transformations [6].

✉ Serena Graziosi
serena.graziosi@polimi.it

1   School of Design, Politecnico di Milano, Via Candiani 72, 20158 Milan, Italy

2   Department of Mechanical Engineering, Politecnico di Milano, Via La Masa 1, 20156 Milan, Italy

3   School of Jewellery, Birmingham City University, Vittoria Street, Birmingham B1 3PA, UK

This paper also deepens this binomial, but it targets a different purpose. Our study does not focus on a specific aspect, i.e. the computational strategy, the bioinspiration, or the description of an iconic design. Instead, through a case study represented by the design of a novel jewellery collection, this study aims to provide a comprehensive perspective on how all these aspects can be systematically linked in a design process to stimulate product and process innovations in jewellery. To develop the computational part of our case study, we have used Rhinoceros with its Grasshopper visual programming environment [12]. It is among the most used platforms for digital modelling in jewellery [13] and a versatile 3D modelling environment [12]. It supports design exploration by allowing the generation of custom scripts but also can count on the availability of multiple plug-ins [14], including those dedicated to jewellery (e.g. Peacock [15] and others, see [12]). However, other general-purpose CAD environments and dedicated software tools can be exploited for jewellery design [11], such as MatrixGold® [16]. Dedicated tools have built-in libraries for specific jewel elements to simplify the modelling phase [11]. However, in our study, we decided not to use a dedicated plug-in or software for jewellery design but to benefit from Grasshopper's computational capabilities and algorithm-based modelling to support parametric design. This and other platforms are already exploited in multiple sectors, from architecture [17] to works in the DfAM field [18–21]. In our study, we took advantage of these computational capabilities to support abstraction, which is at the basis of the model generation, the form-finding process, and the management of changes [22] (related, among others, to the specific AM process selected).

The novelty of our study is threefold. First, in addition to shape complexity, we also exploited functional complexity, i.e. the possibility of printing already assembled mechanisms [1]. There are already examples of jewels exploiting this possibility, such as the *Kinematics* collection [23], developed by the Nervous System studio [5] and printed in nylon via selective laser sintering [23]. There are also fabric-like metal jewels [24] printed via metal AM. However, as underlined in [24], examples of jewels that have harnessed the metal AM design potential are still limited. Therefore, we developed a new jewel collection by exploiting functional complexity with polymer and metal AM. Such a target was reached through bioinspiration and motivated by the intent to explore new interaction modalities between the wearer and the jewel. Besides, shape complexity was also exploited for aesthetic and functional purposes and production-related aspects. Indeed, AM allows having complete control over density. Local density reductions enable control over the weight of the jewel, which is fundamental when evaluating its cost [24, 25]. That added value of AM, especially with precious metals [24], should be further pointed out. AM also allows discriminating the distribution of high- or low-density regions based on aesthetic needs and functional requirements, such as local stiffness and strength of the part [26]. Given the jewel-user interaction, density control can modulate even the acoustic response of the jewel, like what is currently investigated for different materials [27, 28]. All these opportunities have yet to be deeply discussed.

Second, we leveraged functional complexity to create new interaction modalities with the jewel. The paper describes a case study called *Ecdysis*, a 3D-printed jewellery collection inspired by the shape and dynamism of snakes. The *Ecdysis* collection envisions the creation of several dynamic interaction modalities between the user and the jewel by exploiting the behaviour of the ventral scales of the animal. While the dynamism of snakes is already a source of inspiration in soft robotic applications [29, 30], examples in jewellery are still limited and, most importantly, do not fully leverage the available DfAM opportunities. The interaction does not include information communication technology (ICT) content as in *digital jewellery* [31, 32], but it is enabled thanks to the proper combination of DfAM considerations and computational strategies.

Third, we further demonstrated how computational strategies can be used to stimulate new designs, as in [8–10], keep under control the effectiveness of the designed interaction modality, and guarantee that the combination between the shape and its working mechanism is feasible from a manufacturing perspective. The 3D model of the jewel is conceived by parametrising those variables influencing the interaction quality and modality, the product's customisability, and its technical feasibility in printability. This approach, therefore, guarantees the fulfilment of the so-called restrictive design for AM rules [33, 34] and ensures that these rules do not alter the targeted interaction. Besides, these parameters and rules are considered so that multiple fabrication technologies can be used. Multiple versions of a bracelet were generated and 3D-printed using material extrusion (MEX), vat photopolymerisation (VPP), and powder bed fusion (PBF) processes as a further demonstration of the versatility of the implemented digital process. However, it is also worth explaining that in our study we will not explore processability and finishing-related aspects from an experimental point of view. Studies in those fields and related to jewellery are already ongoing, for example, concerning the processability of platinum alloys [35] or other precious materials [36]. In those studies, the shape of the jewel refers to standard or typical designs/samples since those works focus on processing and/or post-processing operations. Our study is instead dedicated to presenting a real case to strengthen the role of AM in jewellery from an engineering design and industrial perspective. Through conventional manufacturing processes, artisans can already give life to unique shapes in high-end jewellery. However, AM technologies can still enhance their work. AM could

allow the creation of easy-to-customise and unique forms within the same production batch. The uniqueness is preserved, although production volumes can be increased, and production flexibility can be extended. Hence, uniqueness can also be democratised, having AM democratised manufacturing [37].

Nevertheless, the interest in AM and precious metal AM is significantly rising [38–40], but still, small laser powder bed fusion (LPBF) machines are considered the ideal solution in this field [41]. Besides, experts are also conscious that the full exploitation of the potential of AM in jewellery demands the development of a new design mindset [38] and awareness of the design and production opportunities available [39]. Therefore, further case studies and examples are needed to allow jewel designers and artisans to exploit AM's potential in their field. The objective is to show how the jewellery industry can significantly extend design and fabrication possibilities by leveraging the synergy between AM technologies and computational design strategies. It is also worth pointing out that to develop the *Ecdysis* collection and thus leverage this synergy, a multidisciplinary team was involved with competencies in the following areas: DfAM and AM technologies, material science, interaction design, and jewel design and manufacturing.

The rest of the paper is structured as follows. Section 2 describes the development process of the Ecdysis collection, starting with an explanation of why new multisensory interaction modalities should be explored in jewellery and how bioinspiration has been implemented. Section 3 summarises the study's contribution and ends the article.

2 Case study: the Ecdysis collection

This section details the process followed to develop the *Ecdysis* collection to fully exploit the potential of 3D printing technology and computational design. First, a reflection on consumers' behaviour as buyers and wearers of jewels was performed to set design and market needs. This analysis identified the snake as the animal that has always played a strategic role in jewellery and the importance of exploring new interaction modalities between the wearer and the jewel. Then, the idea of providing an alternative solution to exploit the iconic role of this animal in jewellery was generated by leveraging the design potential of 3D printing technologies. The challenge was identifying an innovative concept, considering the high number of famous and iconic snake-inspired jewels already available (e.g. see [42]). That solution was found by deepening the characteristic of the animal less exploited in jewellery, which is its way of slithering. This characteristic also matched the need to explore a new form of dynamism for the jewel. Then, the design activity started to render this slithering mechanism into a

jewel both from a functional and shape point of view. Initially, we created a computational model to generate and control a 2D parametric and simplified representation of that mechanism and its main elements. Then, once the variables were set in 2D, we moved to the 3D and finally to the prototyping phase. Multiple 3D printing technologies were tested to gradually validate the solution with polymer 3D printers before moving to the metal one. That approach also demonstrates the generated model's versatility. Indeed, from a reference model, variants were generated to adapt to the specific printing constraints and opportunities. All these reasoning and the related implementing details are described in this section.

2.1 The need for new sensory engagements and interaction modalities and the role of snakes in jewellery

Our sensory channels allow us to elaborate judgements about a product, which is our cognitive response to the product as consumers [43]. Not only are visual or olfactory messages conveyed by the products, but tactile and auditory cues also affect how the consumer appraises the product [44]. The tactile evaluation can overtake visual information, and the *feel-good touch factor* could become an essential marketing aspect [45]. This cognitive response is elaborated starting from three main interconnected aspects [43]: the *Aesthetic Impression*, the *Semantic Interpretation*, and the *Symbolic Association*. The *Aesthetic Impression* is related to the attractiveness or not of a product [43]. The *Semantic Interpretation* refers to the product's function, use, and qualities [43]. The *Symbolic Association* concerns the product's ability to express the owner's identity [43].

Shapes, style lines, textures, and materials can determine the *Aesthetic Impression* of a jewel. Until now, iconic animal shapes have been mimicked in jewellery by preserving the animals' most recognisable features. In the case of snakes, these features are the head, tongue, and dorsal scales. Great attention is paid to rendering the multi-coloured and iridescence properties typical of the animal's skin. The keratinised scales characterise the animal's appearance and represent the jewel's eye-catching feature. However, snakes have also strongly influenced the *Symbolic Association*. The snake in jewellery has been associated with multiple meanings, including rebirth [46], due to the animal's capability of sloughing the skin. It expresses the capability of the wearers to hypnotise or catch the attention of those looking at them. It thus communicates a strong message of presence on behalf of the person who wears it. Nowadays, even more jewels should be able to express the wearer's personality [47]. Despite scales correlating to self-reported fear of snakes [48], they have always played a central role in jewellery design for their symbolic meaning. Concerning the

Semantic Interpretation, particularly the interaction between the wearer and the jewel, some snake-inspired jewels are flexible, thanks to metallic spring-based mechanisms. This flexibility allows wearers to easily roll up the jewel around the wrist or the neck, as the animal would. The jewel's flexibility enables them to interact physically with it, creating a correlation between their actions, the jewel's response, and how it perfectly adheres to their body. However, although snakes have strongly influenced the *Aesthetic Impression* and the *Symbolic Interpretation* of jewels, their influence on the *Semantic Interpretation* could be further leveraged by, for example, exploring new interaction modalities.

If we reflect further on how people interact with jewels, we can easily recognise common patterns regarding gestures and movements. A bracelet, as well as a ring and a necklace, is not just interacting with the body as a surface to decorate, but the act of wearing it requires an engagement that would entice us "into the haptic realm" ([49] p. 40). This haptic interaction would involve elements of friction and effort, inviting the users "to register the consequences of their actions" ([49], p. 40). During the shopping experience, customers keep moving the items they wear to see them better and check how shiny and shimmery they are, as a playful interaction [50, 51]. They turn their wrist repeatedly before buying a ring or a bracelet. The jewel responds to the wearer's input mainly through visual, tactile (also influenced by the material and texture), and, in some cases, auditory cues. A jewel should thus be designed to invite the person who wears it to touch and move it spontaneously as if it were a de-stressing object. Besides, the clasping of the wrist is a natural action that can be made even in the dark with good precision [52]. In addition, the wrist naturally affords rotation [52]. Hence, people usually wear a bracelet on the non-dominant wrist and use the dominant hand to interact with it [52]. They can touch, clamp, and make it slither on the wrist. The movements of a jewel can be unpredictable when they autonomously follow and adapt themselves to the wearer's body actions or, on the contrary, the wearer can fully control them.

Hence, considering how snakes are fundamental for influencing both the *Aesthetic Impression* and the *Symbolic Interpretation* of jewels and how their role in influencing the *Semantic Interpretation* could be more intensely exploited, the Ecdysis collection was ideated and developed. We first started by deepening the animal behaviour and then reflected on how to transfer such behaviour into a jewellery collection.

2.2 Implementing the bioinspiration

Snakes' movements are versatile, allowing them to adopt the most suitable locomotion system according to specific situations [53, 54]. The terrestrial lateral undulation on non-sliding surfaces is the most iconic snake movement.

During this movement, which is possible when a bottom non-sliding surface can support the whole mass, all the points of the snake move simultaneously, following the same path along the snake's length and with a correspondence between wave propagation and forward speed [54]. The snake's skin is a combination of rigid and soft inter-scale zones, responsible for providing flexibility and mechanical resistance to the animal [55] and whose cyclic shedding process is called *ecdysis* [56]. Snake scales are usually differentiated into head, dorsal, and ventral (Fig. 1a). Dorsal scales are small-sized and arranged in rows perpendicular to the snake axis [57]. They are usually more frequently reproduced in snake-inspired jewels because they determine the visual appearance of the animal [54]. They are also on the bottom side of the snake's body (Fig. 1a). However, the scales that play a central role in the snake's locomotion ability are not the dorsal but the ventral ones [58].

The ventral scales have an elongated hexagonal shape [59] (Fig. 1a), with varying aspect ratios (Fig. 1b) [59]. They are bigger than dorsal scales and generally homogeneous in colour and appearance but not in dimensions because bigger scales are placed in heavier sections of the snake's body [59]. This variable aspect ratio (Fig. 1b) determines the friction coefficient variability of the bottom part of the snake's body [59]. In terrestrial snakes, they ensure the contact of the snake to the ground. Some functional inhomogeneities and anisotropies could be observed at the microscopical level. They vary depending on specific movement functions [60]. The number of ventral scales has been recently demonstrated to have, in some species, a 1:1 correlation with the number of vertebrae of snakes [61], which, on the other hand, are connected to some of the muscles responsible for snakes' movements. Despite their crucial role in determining snake movements, the ventral scales have not played the same relevant role in jewels until now. They are not considered the most distinguishing feature of the animal, being not visible, except when the animal, particularly cobras, lifts the head during defensive actions to show their neck [62, 63].

However, considering their crucial function in the snake's slithering on the ground, we decided to investigate further how to mimic their functionalities into a jewel; i.e. the jewel should behave like a snake that, instead of slithering on the ground, is slithering on the wearer's body.

As explained, the snake interacts with the ground through the ventral scales. The head is usually at the same level as the body except during defensive actions [62, 63]. Hence, the wearer's dominant hand (or any surface of the human body where the jewel is placed) and the ground (or any surface where the animal typically slithers) play similar roles in enabling the movements of the jewel (for the wearer) and the ventral scales (for the snake). Hence, since the bracelet and, more generally, the jewel in our collection are the animal,
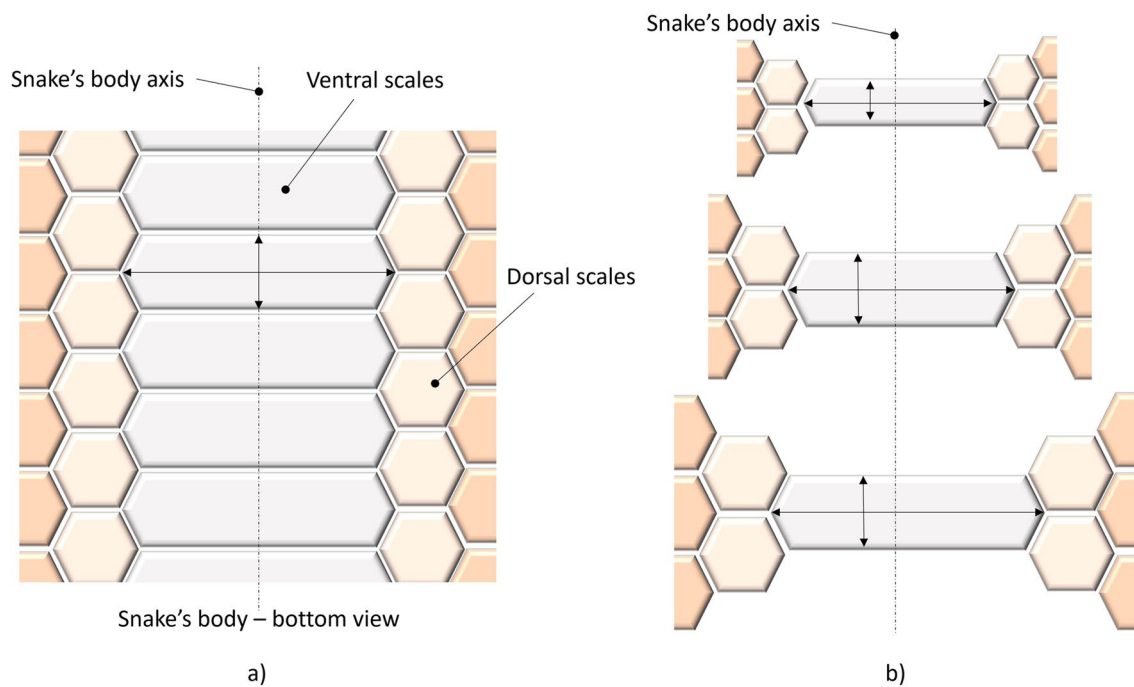
Fig. 1 A graphical representation of the snake's body bottom view with its ventral and dorsal scales. **a** How the scales are shaped and positioned. **b** How the aspect ratio of the ventral scales could vary along the snake's body axis. Images inspired by [58, 59]

like the animal, they should be able to transform themselves dynamically and continuously.

Starting from these further considerations, the *Ecdysis* collection was designed. It consists of several static bracelets, rings, and a kinetic and interactive bracelet: sketches related to the static and dynamic versions of a bracelet are shown in Fig. 2, while further details are provided in the following sub-sections.

2.3 Main design targets and embodiment design

The *Ecdysis* collection is conceived to mimic the function of the snake's ventral scales and evoke the iridescence phenomenon of the snake's skin. To this aim, scales were created as separate but overlapping elements (i.e. moduli), as in the snake, whose three-dimensional texture should be designed to enable it to hide or show different parts and colours, according to the observer's point of view. In the kinetic version, the movements of the modules should be allowed by the touching, clamping, and slithering actions operated by the dominant hand, as it occurs due to friction when the snake's ventral scales slither on the ground. These modules are thus conceived as slightly superimposed to implement a "domino" effect, leading to their simultaneous and progressive rotation once stimulated by the dominant hand.

As the study intends to create an innovative 3D-printed bioinspired collection of jewels and exploits the potentiality

of AM and computational approaches in this field, we paid attention to the following aspects.

Concerning how to physically render the ventral scale behaviour, the problem was initially simplified as a 2D planar representation, and multiple virtual tests and small-scale virtual prototypes were modelled. Figure 3a summarises some initial experiments performed using the Grasshopper environment of Rhinoceros [12] and a combination of commands that allows the creation of a twisting effect (implementing details are provided in Sect. 2.4). This effect was considered the potential solution for mimicking the ventral scale geometry (Fig. 3b) and enabling the dynamics of the jewel. A further fascinating aspect of this effect is the visual cues it triggers (Fig. 3a), which seem to recreate the iridescence characterising the snake's skin. Indeed, some snake species look iridescent, such as the rainbow boa, sunbeam, and indigo snake [64]. Their bright glint is caused by a complex and dynamic physiological process, which leads to a rapid change in pigment and patterns [65]. As the reproduction of this physiological process is not feasible with the currently available AM materials and technologies, we decided to render this dynamic effect through a three-dimensional texture enabled by this twisting pattern and the possibility of generating the scales as separate but interlinked modules (Fig. 3).

Concerning 3D printing, we consider the possibility of implementing the following design heuristics for AM [66]: (1) *customisation* to adapt the jewel to the wearer's

Fig. 2 Sketches of some elements of the Ecdysis collection. **a** Static bracelet. **b** Kinetic bracelet
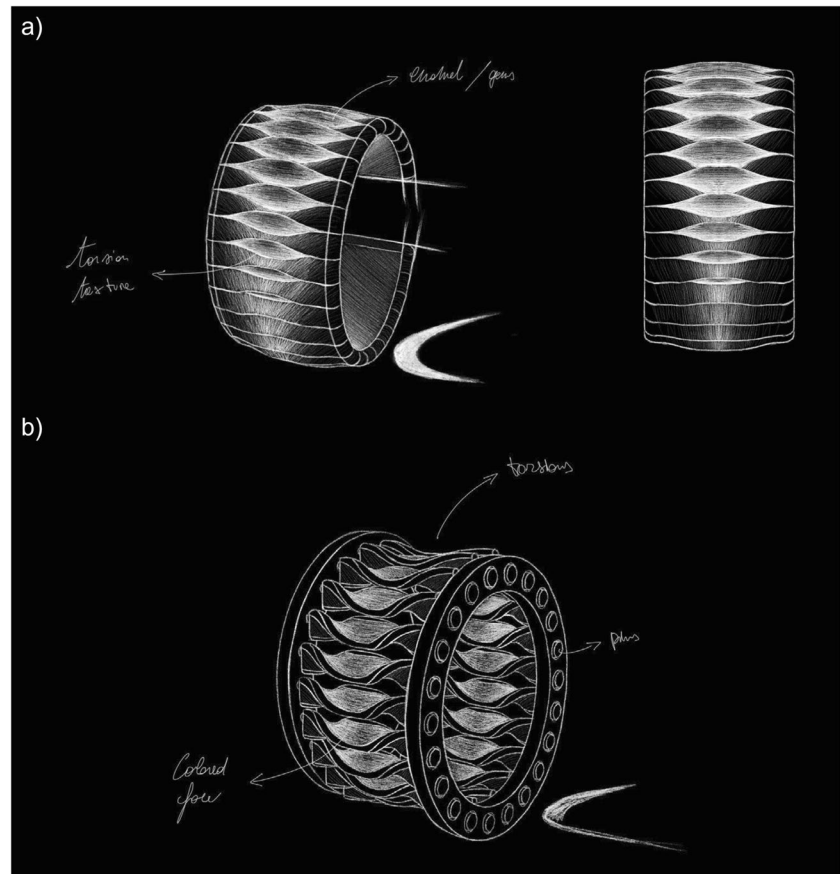
anthropometric characteristics; (2) *part consolidation* to reduce the jewel assembly time; (3) *lightweight* for product wearability, especially in the case of precious metal jewels; (4) *material distribution* to guarantee the relative movements of the jewel's elements and fulfil specific density requirements; and (5) *convey information*, i.e. exploiting the DfAM freedom to mimic the main distinguishing characteristics of the scales also to arouse the *Aesthetic Impression*. Another crucial point was the manufacturability of the proposed collection through multiple AM technologies, which implies the definition of dedicated constraints that, in turn, influence the design process to allow the creation of prototypes. Finally, because AM technologies allow the so-called mass-customisation of the product, it was considered fundamental not only elaborating a dedicated set of variables controlling the generation of multiple product configurations but also properly mastering the influence of these changes on the product manufacturability.

Finally, it is worth mentioning that although the main objective of the design activity was to create an interactive jewels collection, we also developed the static version. We discovered that the twisting effect (Fig. 3) in its static condition was also appropriate to mimic the defensive action of the snake, during which the animal lifts its head and shows its ventral neck scales.

2.4 The computational model

For the sake of simplicity, here we focus the discussion on the computational model of the kinetic bracelet (Fig. 2b). This one consists of two plates connected by the modules representing the ventral scales. The modules do not faithfully replicate the ventral scales morphology; however, the shape of the modules reminds them through a series of aligned torsions (Figs. 2 and 3). The torsion of the modules is not applied to replicate any twist of the ventral scales. In contrast, it is a way to visually remind the snakes' sinuous movements by juxtaposing the hexagonal ventral scales and the rhomboid dorsal ones (Fig. 3b) and creating a play of colours that resembles the iridescence phenomenon. Beyond the twist of the modules, which allows a static representation of the scale morphology, the other key aspect of the jewel is its motion design: it should mimic one of a snake and allow human-jewel interaction.

As mentioned, the computational model was developed within the Grasshopper environment of Rhinoceros. The first step was to identify the main elements of the model and how they are linked. Based on some preliminary evaluations and attempts, we identified ten groups that were clustered into four categories (Table 1): *Shape*, *Customisation*, *Feature imitation and interaction*, and

Fig. 3 The 2D twisting pattern generated through the Grasshopper environment (**a**) and how this pattern is used to mimic the shape of the ventral scales (**b**) shown in Fig. 1
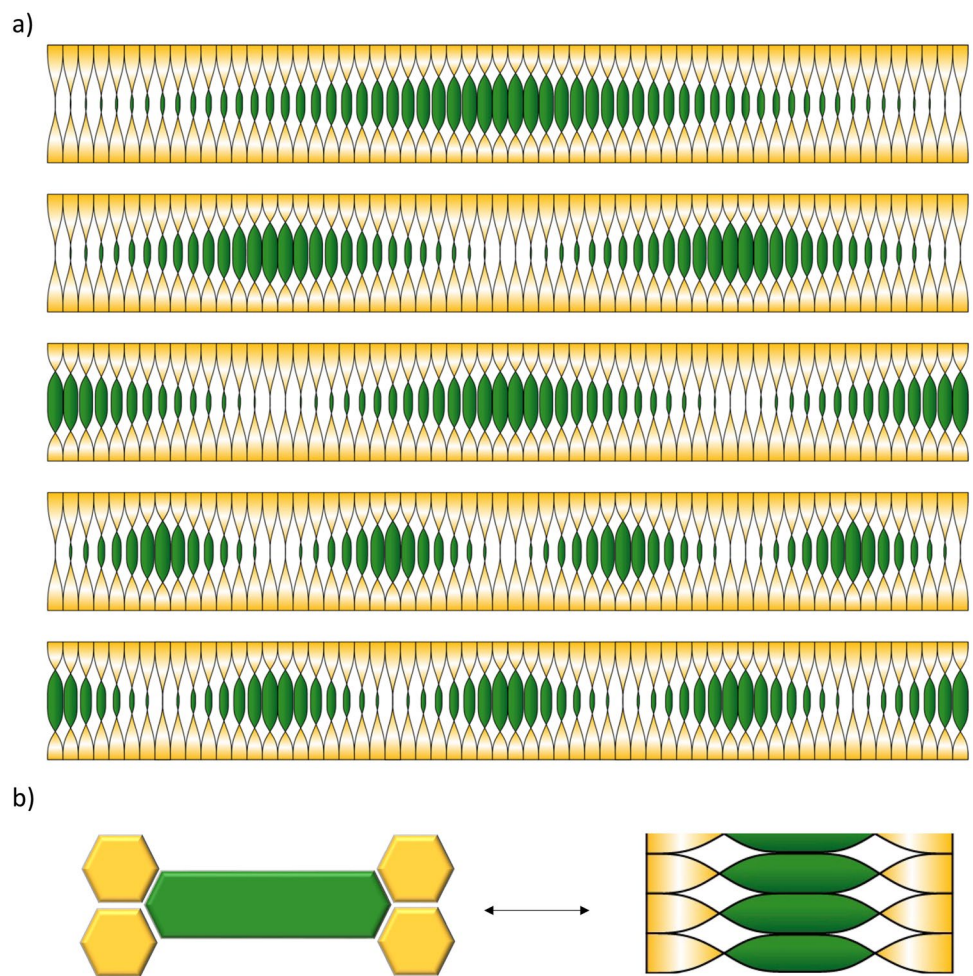

Table 1 The four categories and the ten groups defined for the developed computational model

Category	Group
Shape	Jewel silhouette
	Modules generation
	Pins
	Plates
Customisation	Body sizes
	Modules dimensioning
Feature imitation and interaction	Torsion
	Mechanism of motion
	Colour
Manufacturability	Pin-hole joint

Manufacturability. This classification is the strategy followed to organise the algorithm, even if it is evident that some choices surpass the limits of a single group. The *Shape* category oversees the shape complexity dimension. Hence, within this category are assigned the groups that control the generation of the shape of the main elements of the jewel. The *Customisation* category concerns the main variables that must be changed to adapt the jewel to the wearer's body. The *Feature imitation and interaction* represents the functional complexity dimension in combination with the bioinspiration. It integrates the groups determining the capability of the jewel to render the slithering mechanism correctly and the simulated iridescent effect. *Manufacturability* is focused on guaranteeing the printability of the jewel as pre-assembled. It is, therefore, aimed at managing the pin-hole joint because it is responsible for the movements of the modules. The values assigned to the geometry also influence manufacturability; hence, the groups and, specifically, the variables defined within them are strongly interlinked (Fig. 4a). An overview of the whole Grasshopper model is provided in Fig. 4b. Some Grasshopper components were clustered to facilitate the comprehension of the relationships between the model groups. The full algorithm is available upon request from the corresponding author. Further implementing details are provided later.
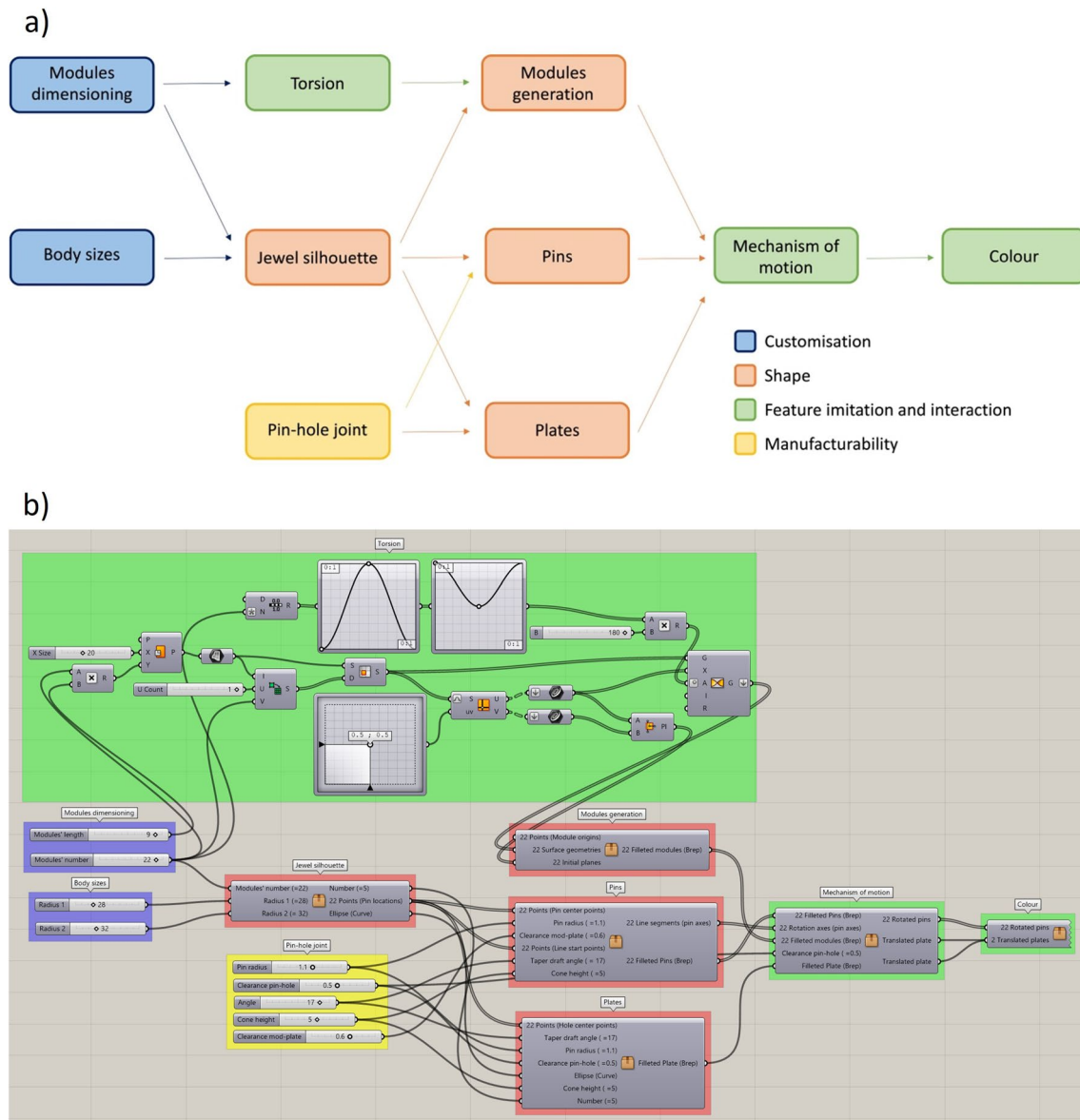
Fig. 4 Overview of the computational model through its ten groups: schematic view (**a**) and Grasshopper model (**b**). Four categories have been identified, highlighted with different colours: *Customisation* (in blue), which contains the "Body sizes" and "Modules dimensioning" groups; *Shape* (in red), which includes "Plates", "Modules generation", "Pins", and "Jewel silhouette"; *Feature imitation and interaction* (in green), which contains the "Torsion", "Mechanism of motion" and "Colour" groups; and *Manufacturability* (in yellow), which coincides with the "Pin-hole joint" group. The links among these groups are highlighted through arrows in the schematic view (**a**). In (**b**), some Grasshopper components were clustered based on the schematic view in (**a**) to facilitate the model comprehension

2.4.1 The "Body sizes" and "Modules dimensioning" groups

The *Customisation* category considers two groups: "Body sizes" and "Modules dimensioning". They allow the definition of the parameters that control the bracelet size. An elliptic profile was chosen instead of a circular one since it fits the wrist shape better. The size can be modified by adjusting the two radius dimensions (Fig. 5a**,** in millimetres) to obtain a perfectly tailor-made jewel instead of just selecting standard sizes. The modules' number and length are the

other essential parameters for defining the overall bracelet dimensions (Fig. 5a, in millimetres). These variables have been treated as input for the computational model.

2.4.2 The "Jewel silhouette" group

The four parameters defined in the *Customisation* category are the inputs of the "Jewel silhouette" group, which belongs to the *Shape* category (Table 1). In this group, the elliptical selected for the jewel is designed. The geometrical entities
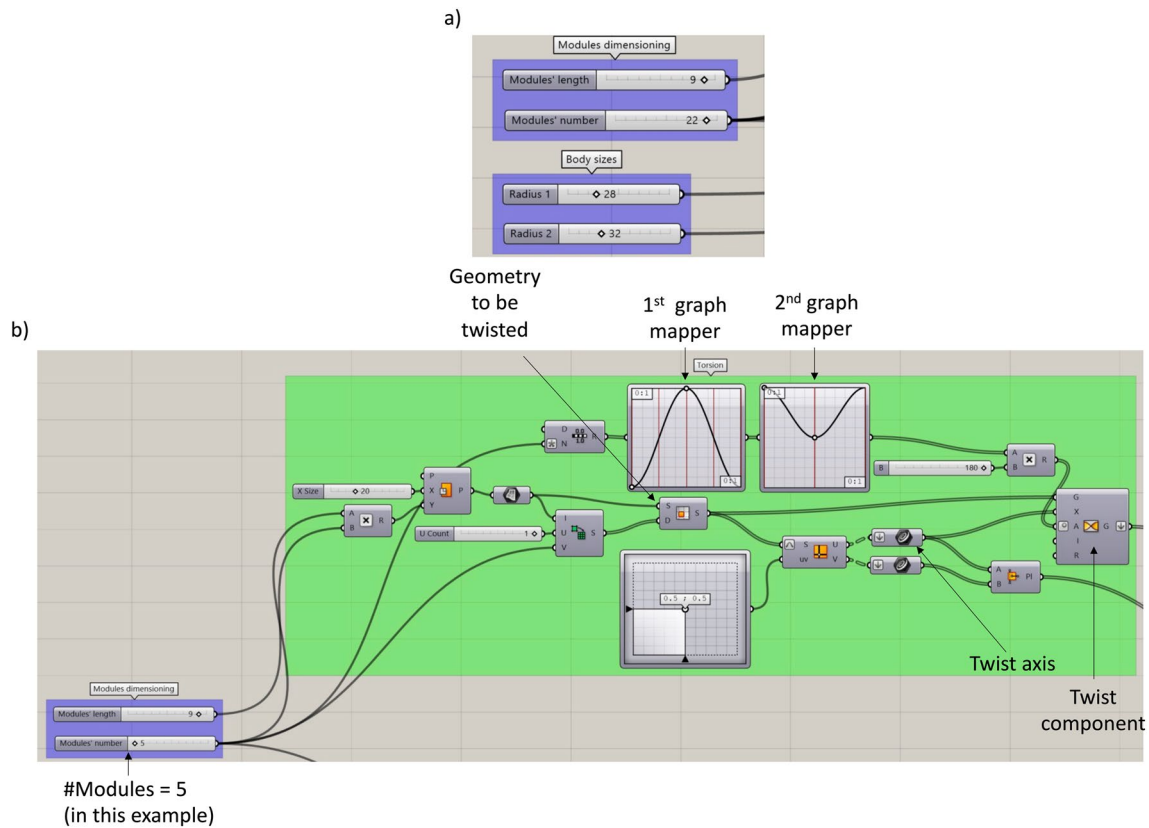
Fig. 5 The "Modules dimensioning", the "Body sizes", and the "Torsion" groups. **a** Number sliders allow changing four parameters (the two radii of the elliptic shape, the modules' length, and number), obtaining a perfectly tailor-made jewel. Length and radii are expressed in millimetres. **b** The "Torsion" group, exploiting the Grasshopper "Twist" component, allows the design of the module's shape. Size and length are expressed in millimetres

defined are the inputs of the other three geometrical groups, in which the plates, the pins, and the modules are designed (Table 1).

2.4.3 The "Torsion" group

The peculiar shape of the modules is obtained inside the "Torsion" group (Fig. 5b), whose inputs are the two modules' parameters already defined. To explain how the modules were designed, the number of modules, called N and equal to 22 in the 3D-printed prototype (Fig. 5a), was set equal to 5 in this example (*Modules' number* in Fig. 5b). The Grasshopper component, which allows deforming objects by twisting them around an axis is called "Twist" (Fig. 5b). Its main inputs are the base geometry to be twisted, the twist axis, and the twist angle (which can be expressed in degrees or radians). Each input can be changed independently from the others. The geometry to be twisted was designed as a set of N adjacent rectangles, whose two dimensions were defined according to the desired dimensions of the bracelet. The longitudinal axis was determined for each rectangle

(Fig. 6a). It is the twist axis input of the "Twist" component (Fig. 5b).

The tricky part was the definition of the twist angle set. A range of N equally spaced numbers is defined in the domain [0;1] to obtain a gradual torsion of the modules. In this simplified example, the set is {0; 0.25; 0.5; 0.75; 1}. By using these values times 180 to obtain an angle value in degrees, as angles input in the twist, the obtained result is a progressive torsion by {0°; 45°; 90°; 135°; 180°} of the five modules (Fig. 6b). Once the twist of the modules is completed, the next step would be their wrapping around the elliptical shape. However, the current configuration (Fig. 6b) is unsuitable for this operation. Even if there is a gradual torsion from module #1 to #5, the transition from #5 to #1 is discontinuous. For this reason, the set of angles was remapped using a first sinusoidal function, shown in Fig. 5b (1st graph mapper). This function is symmetric with respect to the midpoint of the domain [0;1], is equal to 0 at the two extremities, and reaches its maximum (1) at the midpoint ($x = 0.5$). Practically, considering the set previously defined {0; 0.25; 0.5; 0.75; 1} and remapping it, the set {0; 0.5; 1;
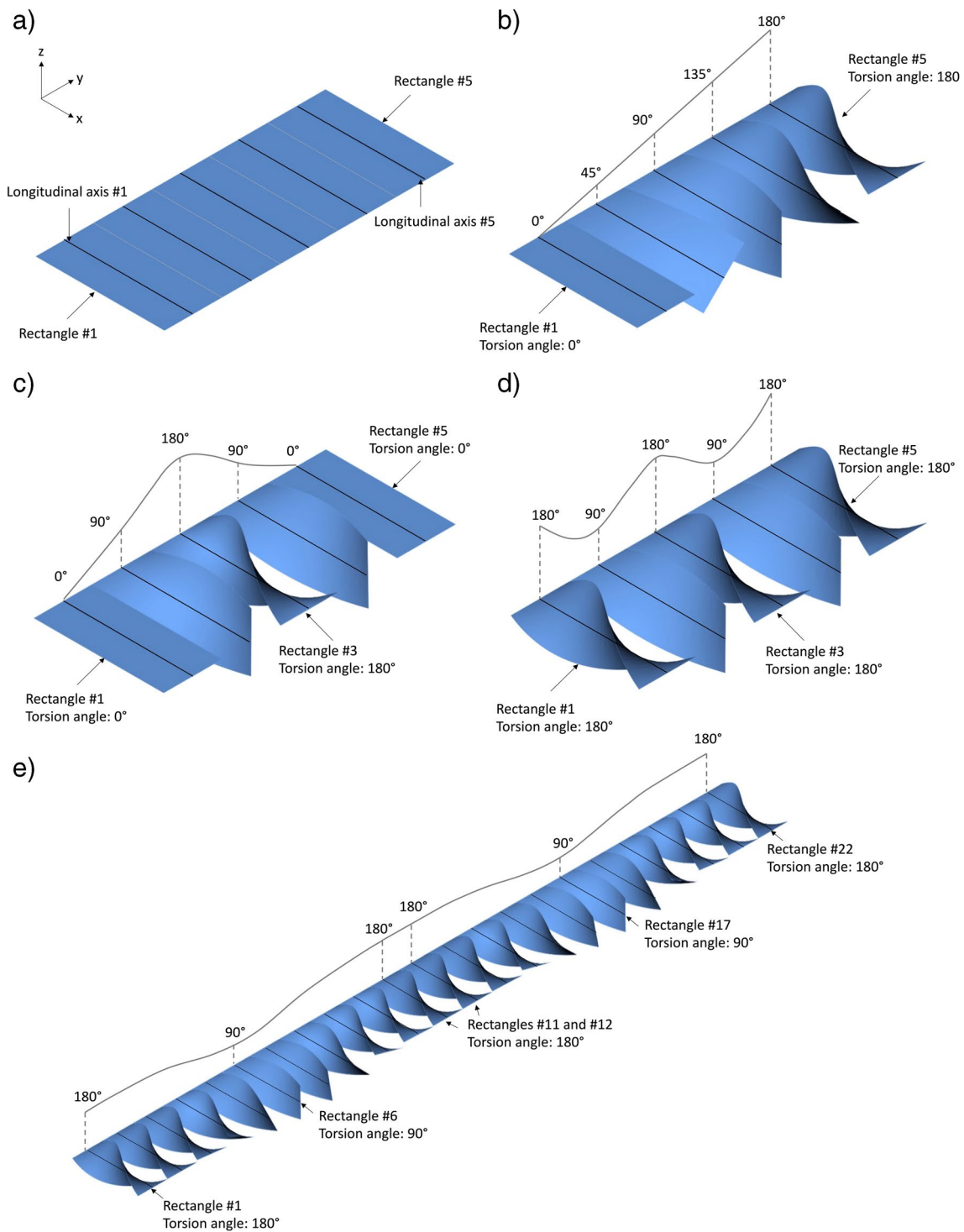
Fig. 6 Steps of the twisting process (isometric views). **a** The geometry used as input in the "Twist" component (a set of $N=5$ adjacent rectangles) and twist axis (the related set of the $N=5$ longitudinal axes of the rectangles). **b** Resulting twist of the geometry (**a**) considering as twist inputs the angles {0°; 45°; 90°; 135°; 180°}. **c** Resulting twist of the geometry (**a**) considering as twist inputs the angles {0°; 90°; 180°; 90°; 0°} obtained through the 1st graph mapper (Fig. 5b). **d** Resulting twist of the geometry (**a**) considering as twist inputs the angles {180°; 90°; 180°; 90°; 180°} obtained through the combination of the 1st and 2nd graph mappers (Fig. 5b). **e** Resulting twist of the geometry considering $N=22$ modules

0.5; 0} is obtained, which corresponds to twisting angles equal to {0°; 90°; 180°; 90°; 0°} (Fig. 6c).

Even if this remap solved the problem of closing the elliptical shape, the juxtaposition of two modules with no torsion is not favourable for transmitting motion from one module to the next. For this reason, a second remap was performed using the sinusoidal function shown in Fig. 5b (2nd graph mapper). Analogously to the previous one, this function is symmetric with respect to the midpoint of the domain; differently, it is equal to 1 at the two extremities and reaches its minimum at the midpoint ($x = 0$). The minimum value is equal to 0.5 (meaning that the amplitude of this function is half of that of the previous one). The effect of this remapping is twofold: on the one hand, it removes all the modules with no twist; on the other, it allows the continuity of the wrapped configuration. The resulting sets are indeed {1; 0.5; 1; 0.5; 1} in the domain [0;1], which corresponds to {180°; 90°; 180°; 90°; 180°} (Fig. 6d). This algorithm works with different numbers of modules. In the kinetic 3D-printed bracelet, N was set equal to 22. The isometric view of the output of the Torsion group is shown in Fig. 6e.

2.4.4 The "Modules generation" group

The output of the "Torsion" group is shown in Fig. 6e, and it is one of the primary inputs of the "Modules generation" group (Fig. 4a), in which the geometry of the modules is created.

The first step is wrapping the half module's surfaces around the ellipse representing the wrist. The objective is to create a closed shape. This is done by first creating a new set of planes perpendicular to the y-axis and having as origin 22 equally spaced points on the wrist size ellipse (defined on the z-y plane); then, through the Grasshopper "Orient" component, the set of 22 geometries shown in Fig. 6e is remapped from the initial set of planes to the final one (Fig. 7a). The second step mirrors the half module design to obtain a symmetric central configuration. Before mirroring, a central transition rectangle was added (Fig. 7b). It increases the contact area between the module and the wrist skin during the jewel rotation and, at the same time, contributes to mimic the shape of the ventral scales (Fig. 3b). The resulting geometry is shown in Fig. 7b. The third step is to offset the module surfaces to obtain solids, as shown in Fig. 7c. In addition, filleting was applied on selected edges to smooth the shape of the modules.

2.4.5 The "Pin-hole joint" group

The *Manufacturability* contains the "Pin-hole joint" group. The connection between the central configuration and the two plates was properly conceived to connect each module to the others and make them roll around their axis. This

connection must satisfy several requirements. First, it should allow the rotation of each module around its axis. Secondly, the rotation of one module should cause the synchronous rotation of all the others. A pin-hole joint with a truncated conic shape was selected, whose parameters were defined in this group and are shown in Fig. 8a. The pins were connected to the modules. To this aim, holes were designed in the two plates. The truncated cone, being axisymmetric, permits the rotation of the pin inside the respective hole. A clearance value (*clearance pin-hole* in Fig. 8a, b) is defined to tailor the distance between each pin and the relative hole. A slightly different value (*clearance mod-plate* in Fig. 8a, b) was set to tailor the distance between the plate and the modules. These values can be adjusted according to the chosen 3D printing technology and material. In this group, other variables, such as the pin radius (*pin radius* in Fig. 8a, b), cone angle (*angle* in Fig. 8a, b), and cone height (*cone height* in Fig. 8a, b), were established. The connection between the module and the respective pin was obtained through a cylinder whose height equals the *clearance mod-plate* value. To block the axial disassembly of the coupling, the cone angle and the clearance values were chosen to have the hole's minor radius bigger than the pin's major radius (Fig. 8b). The geometry of the pins was also selected to guarantee the printability of the bracelet for the chosen printing orientation.

2.4.6 The "Plates" and "Pin" groups

The other two groups of the *Shape* category are the "Pins" and the "Plates" (Table 1), which depend on the parameters defined in the "Pin-hole joint" and on the geometrical entities defined in the "Jewel silhouette". In these groups, the geometries of the two pierced plates and the pins were created. The plates are fundamental to guarantee the synchronous rotations of the modules.

2.4.7 The "Mechanism of motion" and "Colour" groups

Once the static geometry of the whole bracelet had been obtained and the proper interface between the modules and the plates had been defined, it was necessary to devise the bracelet mechanism of motion. This was done in the "Mechanism of motion" group. First, it is essential to design how to connect the truncated conic pins to the modules. The two pins of each module were not aligned to obtain the synchronised rotation of all the modules. Still, they were positioned staggered with respect to the torsion axis by translating them towards opposite directions (Fig. 8c). This means that to maintain the alignment of each pin with the respective hole, a translation of the two plates in the opposite direction should be applied. This implies that a rotation of the modules around their axis should correspond to a
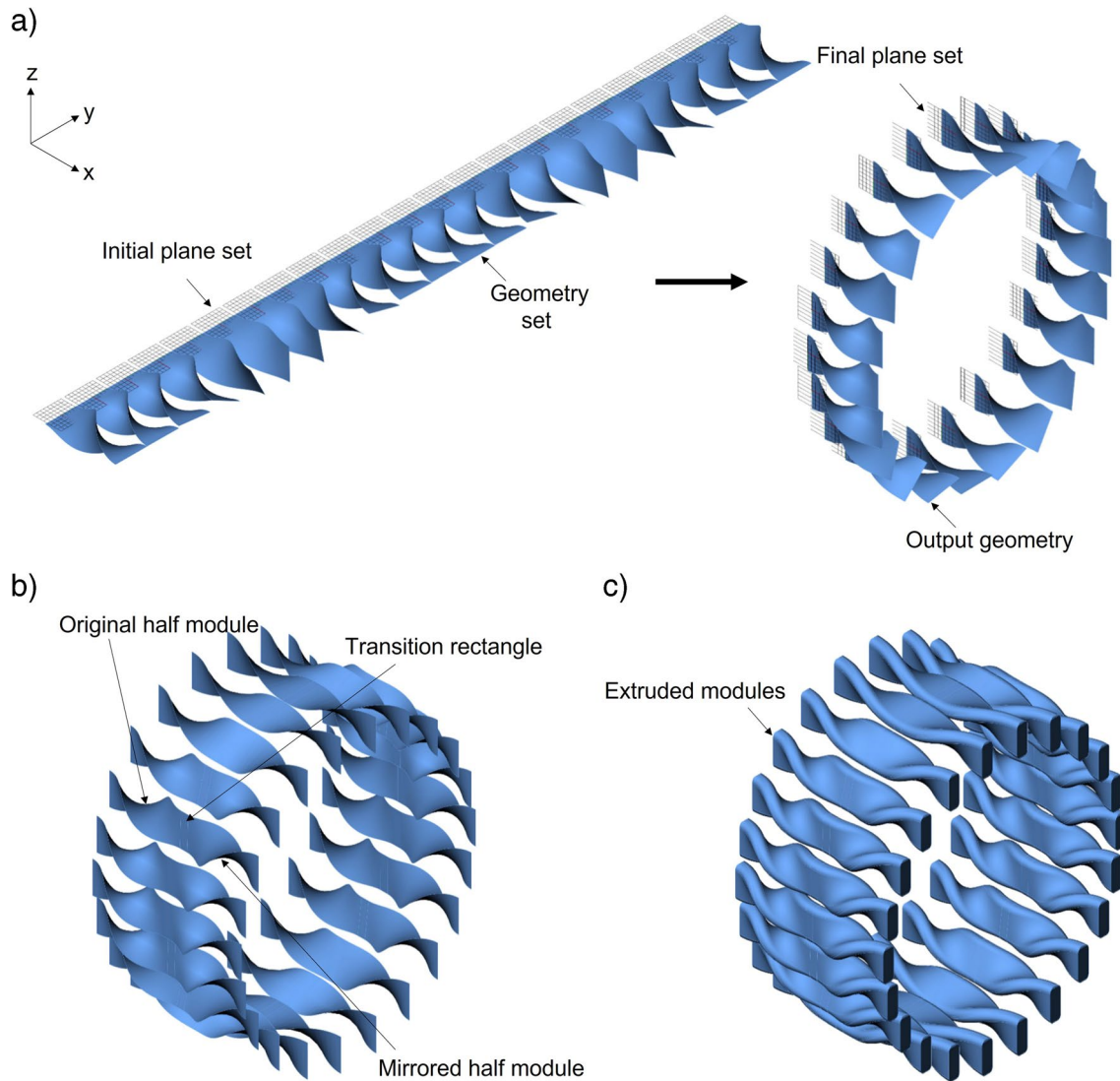
Fig. 7 Steps of the modules' 3D model generation (isometric views). **a** Wrapping of the 22 modules around the wrist size ellipse: the inputs (left) and output (right) of the "Orient" component are shown.

b Design of the transition rectangles and mirroring of the half modules to obtain their entire profile. **c** Extrusion of the modules' profile

rigid translation of the two plates along a circular trajectory, whose radius corresponds to the translation of the pins with respect to the module axis.

To verify the proper mechanism of movement and the effect of the possibility of colouring the jewel surfaces to strengthen the simulated iridescent effect, first, different colours were assigned to the bracelet elements through the "Colour" group: the whole jewel was painted gold, and then, the internal surface of each module was dyed pink. Then, the movement can be visualised through a number slider that acts on the rotation angle of the modules around their axis and simultaneously on the rotation of the vector, controlling the translation of the two plates. The isometric and lateral views of the jewel at four rotation stages are shown in Fig. 9a, b. The Rhinoceros environment also allows for

visualising the motion mechanism before printing the prototype, as shown in Fig. 9c. In the case of the static version of the bracelet, its computational model has a simplified structure compared to the one described above. The "Mechanism of motion" and "Pin-hole joint" groups are not present. The groups related to the shape are modified to obtain the geometry shown in Fig. 2a. Concerning the rings, a 360° elliptical geometry is created. At the same time, for the bracelet, it is also possible to design an open profile (further details in Sect. 2.5) facilitating the wearing.

2.4.8 Generation of multiple configurations

A further aspect to underline concerning the developed computational model is the possibility of customising the jewel
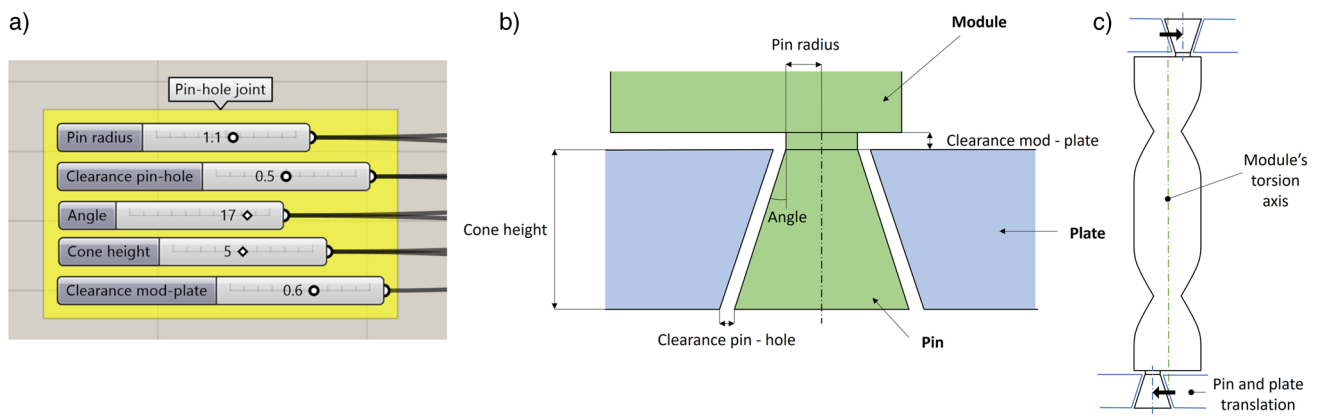
Fig. 8 The "Pin-hole joint" and the "Mechanism of motion" groups. **a** Parameters of the pin-hole clearance coupling (linear dimensions expressed in millimetres, angles in degrees). **b** Representation of the coupling and its parameters. **c** Pin and plate translation with respect to the module's torsion axis


Fig. 9 The mechanism that allows mimicking the snake ventral scale slithering. **a** Isometric views of the jewel at four stages of the rotation (0°, 90°, 180°, and 270°). **b** Lateral views of the entire jewel at the same four stages. It is possible to notice the translation of the two plates along a circular trajectory. **c** A collection of frames (from left to right) shows the kinetic bracelet's working mechanism, i.e. the rotation of the modules around their axis and the synchronous translation of the two plates

and keeping its density under control. In jewellery, density control is essential for cost reasons [26]: different sizes of the same jewel are characterised by different volumes, therefore different weights, and thus different costs, which is, however, something unwanted. For example, three different sizes of the kinetic bracelet with their relative dimensions are shown in Fig. 10a.

The sizing is not merely performed by scaling the jewel; this is fundamental to preserving the jewel's manufacturability, aesthetics, and functionalities in all configurations. To this aim, all the parameters defined in the "Pin-hole joint" group should be kept constant; therefore, only the ellipse's two radii and the modules' length and width can be changed. However, to avoid cost differences among the three configurations, a practical way possible thanks to the freedom

allowed by AM technologies and not, for example, via casting could be to reduce the effective density of medium and large sizes to obtain the same weight and cost of the smaller one. For example, the modules and the plates could be printed as "shells". By setting a wall thickness equal to 0.5 mm and infill densities equal to 0% for the modules and 100% for the two plates, a weight reduction of 34–40% (depending on the selected size) is obtained (Fig. 10b). If a powder-based 3D printing technology is chosen, holes must be designed at the bottom of each module to allow the unfused/unsintered powder to exit from the hollow structures (Fig. 10c). These changes could, for example, influence some acoustic cues the jewel provides. Hence, they should be implemented carefully or in a way that favours specific auditory responses.
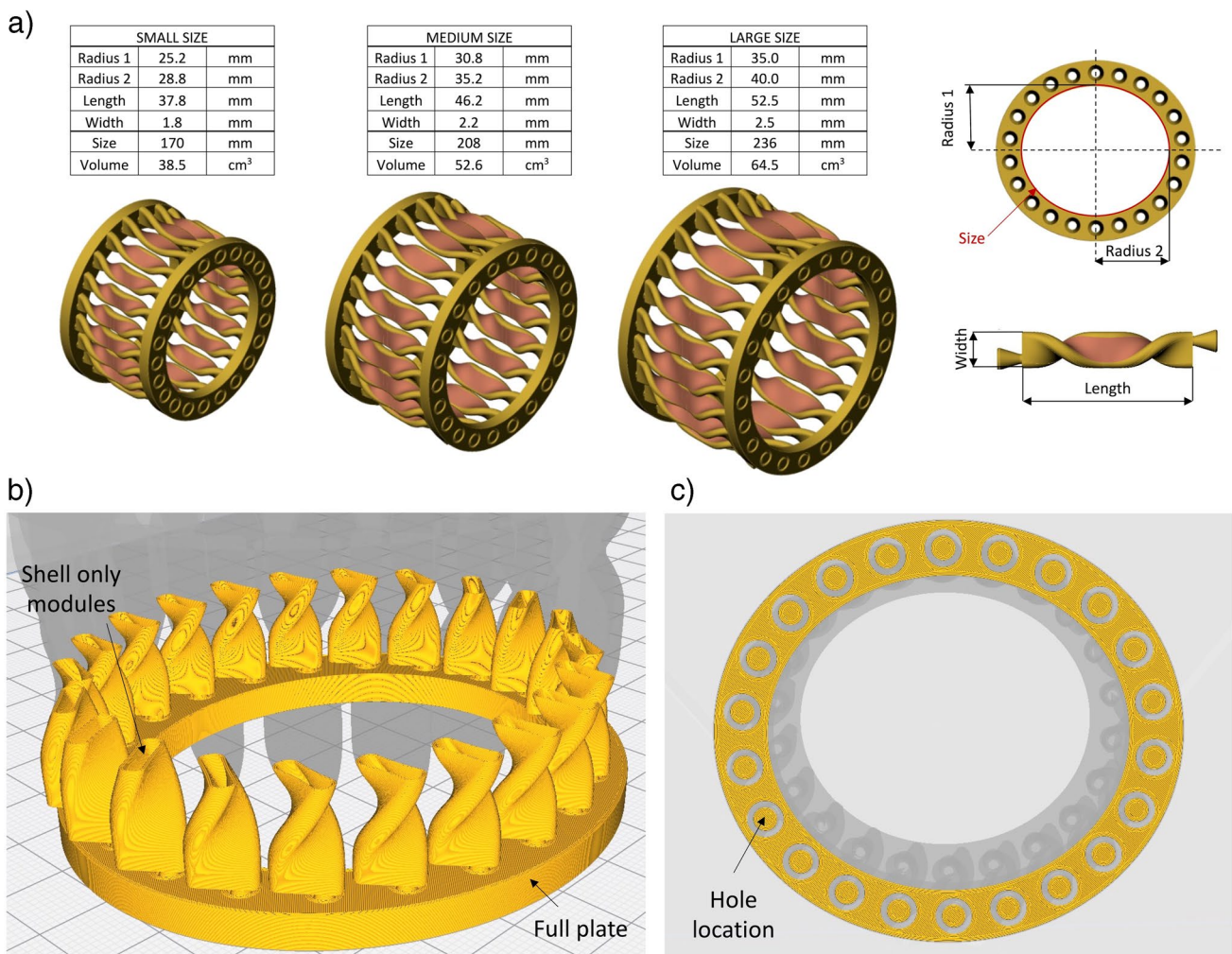
Fig. 10 Sizing of the kinetic bracelet and examples of lightweighting solutions and density control offered by AM technologies. **a** Three different sizes (small, medium, and large) were modelled by changing the four parameters shown in the right part of the figure. The resulting size (perimeter of the internal ellipse of the plate) and total volume are reported in the tables. **b** Selection of different infill densities for the multiple parts of the jewel, such as a shell-only configuration for the modules (wall thickness equal to 0.5 mm) and a 100% infill density for the plates. **c** Bottom holes should be included in the modules to allow the exit of the unfused powder from the hollow structures (in the figure, their potential location is shown)

2.5 3D printing of the polymeric prototype

The kinetic jewel was printed using a stereolithography (SLA) 3D printer. The selected printer is the Form 3B (Formlabs Inc.), and the material is the Clear resin. An orientation with the two plates parallel to the building plate was set. The computational model allows the printing of the jewel as pre-assembled to optimise manufacturing times. Moreover, the gradual torsion of the modules makes them self-supporting during the printing. In any case, support was necessary to sustain the second plate and guarantee the clearance between the module's extremities and the plates. The support volume is approximately 32% of the total printed volume. After the printing, all supports were removed, and the prototypes were painted to mimic a gold jewel. Indeed, to further strengthen the iridescent effect, the two faces of the modules can be finished in two different ways: for example, one surface can be paved with coloured gems, plated with another metal, or even coated with classical enamel or any other covering material. Gold surfaces and gems can also

enhance the visual interaction with the jewel due to their light reflection ability. The final 3D-printed prototypes are shown in Fig. 11a–c.

The prototypes of the static elements of the collection were instead printed using a fused filament fabrication (FFF) 3D printer (Ultimaker S5) and polypropylene (PP) (Fig. 11d). The flexibility of PP allows the narrowing of the dimension of the bracelet opening. Supports were not required, and the jewel was painted analogously to the kinetic version (Fig. 11e, f). The dynamic 3D-printed prototype successfully rotates around the wrist skin when stimulated by the dominant hand, as shown in Fig. 11g.

2.6 3D printing of the metallic jewel

Based on the contribution of an expert in the field, all the jewels were judged as printable in gold with LPBF technologies. The kinetic jewel can be printed either pre-assembled or separated into parts. In this second case, finishing all the surfaces and making them perfect,

Fig. 11 The 3D-printed prototypes of the kinetic and static bracelets. **a** The kinetic bracelet printed with SLA and after support removal. **b–c** The bracelet (**a**) after painting using fingernail polish. **d** The open static bracelet printed with FFF. **e**, **f** The bracelet (**d**) and a ring after painting using fingernail polish. **g** A collection of frames (from left to right) showing how the modules of the bracelet rotate around the wrist skin when stimulated by the dominant hand
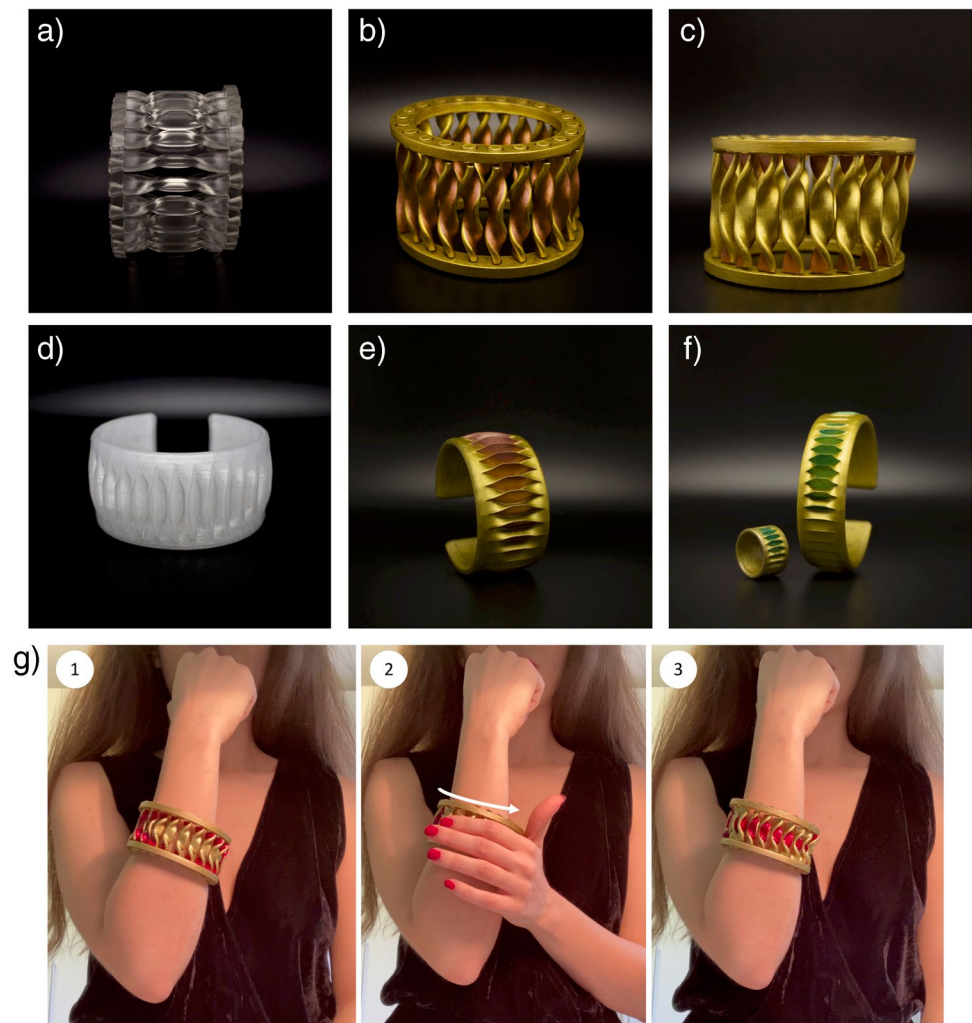
as high-end jewels require, would be easier. However, even if printed as pre-assembled, with supports limited in quantity and placed in not visible zones, their presence represents a little drawback. Hence, we printed the kinetic prototype with a metallic material, specifically bronze, to validate these considerations. Specifically, we printed an intermediate version between the small and the medium sizes (Fig. 10a).

Some changes were implemented to ensure the kinetic model's successful printing as pre-assembled. The following targets drove those changes: (1) reduce the weight of the jewel for more comfortable wearability, (2) guarantee its printability using a powder-based technology, and (3) test an additional aesthetic configuration. The main modifications are summarised in Fig. 12a.

Differently from SLA, the selected printing orientation, to minimise supports and avoid too big cross-sections, was with the bracelet inclined (flat faces parallel to the building plate should be avoided). Fillets were added to the two faces of the modules located near the plates to reduce the number of flat faces. Then, the cross-section of the plates was modified from the original rectangular shape to a more harmonious, almost elliptic one. Cuts in the modules have been performed to reduce their weight and permit the eventual enamel application. Finally, the pin and hole shape has been changed to test a different aesthetic configuration. A clearance value of 0.5 mm was considered to guarantee the relative motion between plates and modules. Thanks to all these changes, weight reductions of 36% and 48% have been achieved for plates and modules, respectively, leading to a whole weight reduction of 43%.

The prototype has been printed using the Sisma MySint100 (Sisma S.p.A., Vicenza, Italy) and the PM-BR101P powder (90% Cu, 10% Sn) by Legor (Legor Group S.p.A., Bressanvido, Italy) with a layer height of 15 μm (laser: 100 W, speed 1200 mm/s). Figure 12b shows the jewel at the end of the printing process; supports, whose volume is around 30% of that of the jewel, were manually removed using hand tools

Fig. 12 The creation of the digital and physical model of the metal bracelet. **a** Changes to the kinetic bracelet to allow its printability using laser powder bed fusion and to test an additional aesthetic configuration. Modules and plate modifications lead to a weight reduction of 48% and 36%, respectively, compared to the initial design. **b**, **c** 3D-printed bronze kinetic bracelet in its "as-built" configuration (**b**) and after post-processing (**c**)
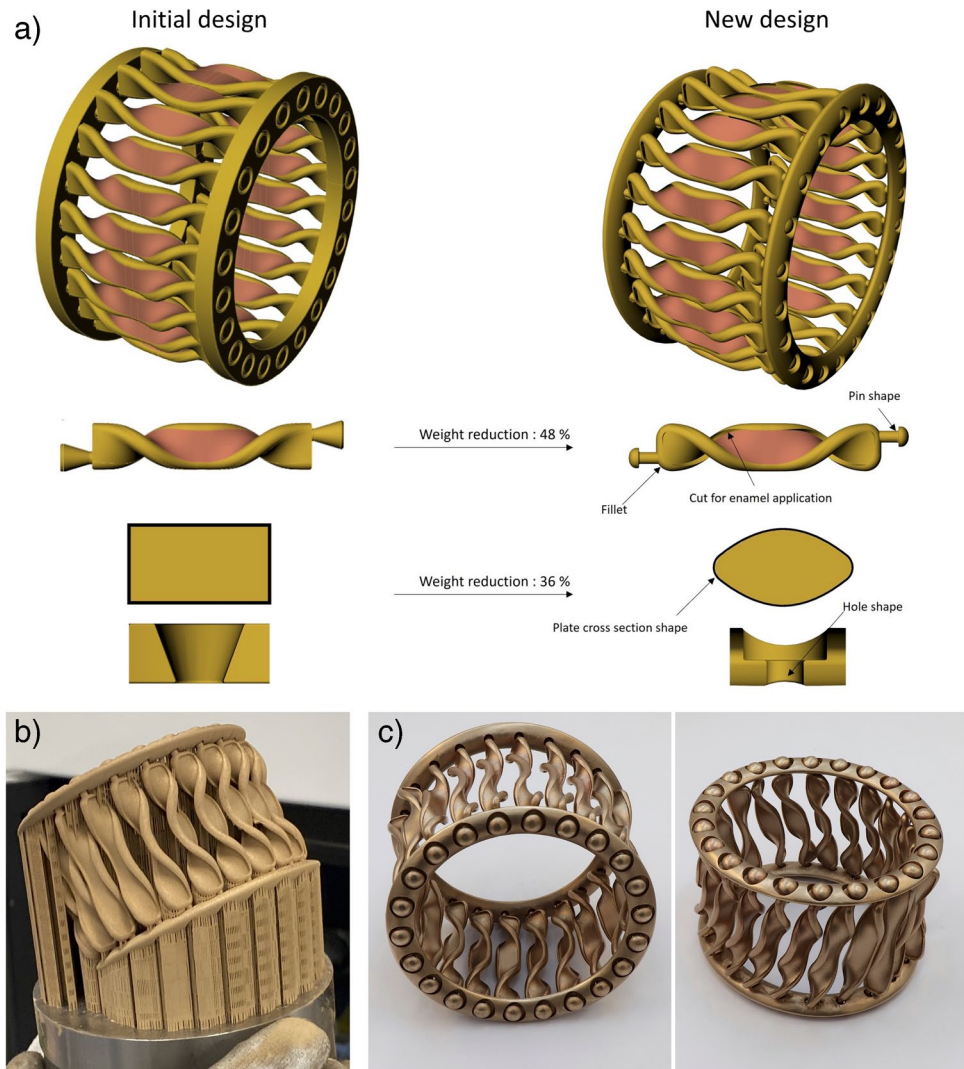
(flush cutters). The bronze prototype, after post-processing, is shown in Fig. 12c. A first finishing step was performed, demonstrating that the overall quality was satisfactory. Besides, the mechanism works properly. The dynamic metallic bracelet also provides the Jingle effect. The analysis of the acoustic response of the bracelet, because of its optimisation/customisation and related to the bracelet material and its geometrical features, including local density reductions, was not part of the present work. However, results demonstrated that this further design aspect could be included in future developments of the computational model.

3 Conclusions

This paper deepens the synergistic role between AM technologies and computational strategies in extending the design and manufacturing boundaries of the jewellery industry. Their integration in the digital design and manufacturing paradigm context promotes the production of unique shapes and unconventional interaction modalities between the jewel and the wearer. We demonstrate this potential through a case study: a 3D-printed bioinspired and interactive jewel collection called *Ecdysis*.

Taking snakes' shape, dynamism, and iridescence as inspiration, this collection was developed starting from a computational model that allows adjusting the jewels' configuration according to the selected printing technology and, more generally, to modify every dimension, detail, and size effortlessly. These "smart" changes would not be manageable without this model. They are not just functional; they can also enhance the design of different but still coherent versions of the jewel that could be part of the collection. They can also be directly modified by those customers who want to personalise the items themselves, enabling mass customisation. This could lead to a new, engaging, and interactive shopping experience in which the customer participates in the design of its one-of-a-kind and exclusive jewel. The concept behind the *Ecdysis* collection has been triggered by the snake's movements and the intent to fully address the consumer's cognitive response based on the *Aesthetic Impression*, the *Semantic Interpretation*, and the *Symbolic Meaning*.

The study aims to highlight that all these opportunities are made possible by combining AM technologies with computational design strategies and tools. Specifically, computational design strategies in jewellery allow capitalising on AM's design and fabrication opportunities. They enable extending design boundaries and mastering the increased complexity in favour of an effective manufacturing process that allows fabricating products as pre-assembled and tuning the material distribution. The possibility of locally controlling the object weight, while it is already capitalised in

other fields (e.g. in aerospace [67]), could also become a distinctive feature of the jewellery sector. A design strategy that allows obtaining a discretional concentration of precious metals based on aesthetics, functionality, and interaction requirements would improve the control of the precious material in specific jewellery parts. This possibility would contribute to using the same amount of precious metal across different sizes and, therefore, would support a more detailed cost and price management, now very often based on compromising across different sizes and related weights. Besides, it would allow tuning important multisensory cues, such as those related to sound, which are essential in jewellery design. This aspect has yet to be addressed in this study, but it could be considered in future work. The development of the case study has also highlighted further relevant aspects. First, a multidisciplinary team is fundamental to properly deal with all the involved design and manufacturing challenges. Even more, considering the increased complexity of what can be created, it is essential to combine the knowledge and competencies of product and process experts and professionals working in the field of DfAM to exploit the design potential of AM technologies. Indeed, the development and implementation of the computational model is not straightforward and requires an initial phase of abstraction of all the aspects involved in the design activity and how they are linked. Hence, it will be fundamental to develop computational methods and frameworks as in [19] to enable the implementation of multidisciplinary design optimisation and concurrent design approaches.

Declarations

References

1. Rosen D, Wong J (2023) Introduction to design for additive manufacturing. In: Additive Manufacturing Design and Applications. ASM International 83–96. https://doi.org/10.31399/asm.hb.v24a.a0006947
2. du Plessis A, Broeckhoven C, Yadroitsava I, Yadroitsev I, Hands CH, Kunju R, Bhate D (2019) Beautiful and functional: a review of biomimetic design in additive manufacturing. Addit Manuf 27:408–427. https://doi.org/10.1016/j.addma.2019.03.033
3. Nervous System (2007) Hyphae jewelry. https://n-e-r-v-o-u-s.com/projects/tags/jewelry/albums/hyphae-jewelry/. Accessed 3 Jan 2024
4. Nervous System (2015) Florescence jewelry. https://n-e-r-v-o-u-s.com/projects/albums/floraform-jewelry/. Accessed 27 Dec 2023
5. Nervous System (2007) About us. https://n-e-r-v-o-u-s.com/about_us.php. Accessed 27 Dec 2023
6. Bader C, Patrick WG, Kolb D, Hays SG, Keating S, Sharma S, Dikovsky D, Belocon B, Weaver JC, Silver PA, Oxman N (2016) Grown, printed, and biologically augmented: an additively manufactured microfluidic wearable, functionally templated for synthetic microbes. 3D Print Addit Manuf 3:79–89. https://doi.org/10.1089/3dp.2016.0027
7. Oxman N (2014) Mushtari, Jupiter's Wanderer. https://neri.media.mit.edu/projects/details/mushtari.html. Accessed 7 Jan 2024
8. Bertacchini F, Pantano PS, Bilotta E (2023) Jewels from chaos: a fascinating journey from abstract forms to physical objects. Chaos 33:013132. https://doi.org/10.1063/5.0130029
9. Bertacchini F, Bilotta E, Demarco F, Pantano P, Scuro C (2021) Multi-objective optimization and rapid prototyping for jewelry industry: methodologies and case studies. Int J Adv Manuf Technol 112:2943–2959. https://doi.org/10.1007/s00170-020-06469-2
10. Di Nicolantonio M, Rossi E, Stella P (2020) Generative design for printable mass customization jewelry products. In: Di Nicolantonio, M., Rossi, E., Alexander, T. (eds) Advances in additive manufacturing, modeling systems and 3D prototyping. AHFE 2019. Advances in Intelligent Systems and Computing, vol 975. Springer, Cham., 143–152. https://doi.org/10.1007/978-3-030-20216-3_14
11. Wannarumon S (2014) Reviews of computer-aided technologies for jewelry design and casting. Naresuan University Engineering Journal 6:45–56. https://doi.org/10.14456/nuej.2011.8
12. Robert McNeel & Associates (2023) Rhinoceros. www.rhino3d.com. Accessed 17 Dec 2023
13. Schwab FA, de Oliveira BF (2019) Jewels mechanics: structural research applied in conception and development. Int J Interact Des Manuf 13:1049–1059. https://doi.org/10.1007/s12008-018-00526-7
14. Holzer D (2016) Design exploration supported by digital tool ecologies. Autom Constr 72:3–8. https://doi.org/10.1016/j.autcon.2016.07.003
15. González Abalde D (2014) Peacock. https://www.food4rhino.com/en/app/peacock. Accessed 27 Dec 2023
16. Gemvision (2023) MatrixGold. https://gemvision.com/matrixgold. Accessed 30 Nov 2023
17. Caetano I, Leitão A (2020) Architecture meets computation: an overview of the evolution of computational design approaches in architecture. Archit Sci Rev 63:165–174. https://doi.org/10.1080/00038628.2019.1680524
18. Veloso F, Gomes-Fonseca J, Morais P, Correia-Pinto J, Pinho ACM, Vilaça JL (2022) Overview of methods and software for the design of functionally graded lattice structures. Adv Eng Mater 24:. https://doi.org/10.1002/adem.202200483
19. Liu G, Xiong Y, Rosen DW (2021) Multidisciplinary design optimization in design for additive manufacturing. J Comput Des Eng 9:128–143. https://doi.org/10.1093/jcde/qwab073
20. Stanković T, Shea K (2020) Investigation of a Voronoi diagram representation for the computational design of additively manufactured discrete lattice structures. J Mech Des 142:. https://doi.org/10.1115/1.4046916
21. Letov N, Zhao YF (2022) A geometric modelling framework to support the design of heterogeneous lattice structures with non-linearly varying geometry. J Comput Des Eng 9:1565–1584. https://doi.org/10.1093/jcde/qwac076
22. Caetano I, Santos L, Leitão A (2020) Computational design in architecture: defining parametric, generative, and algorithmic design. Front Archit Res 9:287–300. https://doi.org/10.1016/j.foar.2019.12.008
23. Nervous System (2013) Kinematics jewelry. https://n-e-r-v-o-u-s.com/projects/albums/kinematics-jewelry/. Accessed 1 Dec 2023
24. Ferraro M (2023) Additive Manufacturing in the jewellery industry: exploring the potential of platinum and titanium. Metal AM 4:139–144
25. Fani V, Falchi C, Bindi B, Bandinelli R (2021) Implementation framework for PLM: a case study in the fashion industry. Int J Adv Manuf Technol 113:435–448. https://doi.org/10.1007/s00170-021-06623-4
26. Ferraro-Cuda M (2017) Can innovative precious metals additive manufacturing (PMAM), disrupt and push the precious jewellery industry in a new technology age? Progresses and evaluations: a comparative analysis of the Italian and the UK industries. MBA Dissertation, University of Winchester
27. Kuschmitz S, Ring TP, Watschke H, Langer SC, Vietor T (2021) Design and additive manufacturing of porous sound absorbers—a machine-learning approach. Materials 14:1747. https://doi.org/10.3390/ma14071747
28. Liu Z, Zhan J, Fard M, Davy JL (2016) Acoustic properties of a porous polycarbonate material produced by additive manufacturing. Mater Lett 181:296–299. https://doi.org/10.1016/j.matlet.2016.06.045
29. Arachchige DDK, Chen Y, Godage IS (2021) Soft robotic snake locomotion: modeling and experimental assessment. In: 2021 IEEE 17th International Conference on Automation Science and Engineering (CASE). IEEE, 805–810. https://doi.org/10.1109/CASE49439.2021.9551398
30. Wang C, Puranam VR, Misra S, Venkiteswaran VK (2022) A snake-inspired multi-segmented magnetic soft robot towards medical applications. IEEE Robot Autom Lett 7:5795–5802. https://doi.org/10.1109/LRA.2022.3160753
31. Fortmann J, Heuten W, Boll S (2015) User requirements for digital jewellery. In: Proceedings of the 2015 British HCI Conference. ACM, New York, NY, pp 119–125 https://doi.org/10.1145/2783446.2783573
32. Wallace J, Dearden A (2005) Digital jewellery as experience. Future Interaction Design. Springer-Verlag, London, pp 193–216
33. Laverne F, Segonds F, Anwer N, Le Coq M (2015) Assembly based methods to support product Innovation In Design For Additive Manufacturing: An Exploratory Case Study. Journal of Mechanical Design 137:. https://doi.org/10.1115/1.4031589
34. Pei E, Rosen DW, Seepersad C (2023) Design rules. In: Additive manufacturing design and applications. ASM International 97–115. https://doi.org/10.31399/asm.hb.v24A.a0006948
35. Klotz UE, König FR (2023) Additive manufacturing of platinum alloys : practical aspects during laser powder bed fusion of jewellery items. Johnson Matthey Technol Rev 67:303–316. https://doi.org/10.1595/205651323X16691084445762

36. Sohrabi N, Jhabvala J, Kurtuldu G, Frison R, Parrilli A, Stoica M, Neels A, Löffler JF, Logé RE (2021) Additive manufacturing of a precious bulk metallic glass. Appl Mater Today 24:101080. https://doi.org/10.1016/j.apmt.2021.101080

37. Simpson TW, Williams CB, Hripko M (2017) Preparing industry for additive manufacturing and its applications: summary & recommendations from a National Science Foundation workshop. Addit Manuf 13:166–178. https://doi.org/10.1016/j.addma.2016.08.002

38. Ferraro-Cuda M (2020) Innovation and differentiation: precious metal additive manufacturing in the jewellery sector. Metal AM 6:107–117

39. Cooper F (2016) Sintering and additive manufacturing: "additive manufacturing and the new paradigm for the jewellery manufacturer." Prog Addit Manuf 1:29–43. https://doi.org/10.1007/s40964-015-0003-2

40. Yap YL, Yeong WY (2014) Additive manufacture of fashion and jewellery products: a mini review. Virtual Phys Prototyp 9:195–201. https://doi.org/10.1080/17452759.2014.938993

41. Khorasani A, Gibson I, Veetil JK, Ghasemi AH (2020) A review of technological improvements in laser-based powder bed fusion of metal printers. Int J Adv Manuf Technol 108:191–209. https://doi.org/10.1007/s00170-020-05361-3

42. Bulgari (2017) Bulgari icons. https://www.bulgari.com/en-int/bulgari-heritage-icons.html. Accessed 14 Jun 2023

43. Crilly N, Moultrie J, Clarkson PJ (2004) Seeing things: consumer response to the visual domain in product design. Des Stud 25:547–577. https://doi.org/10.1016/j.destud.2004.03.001

44. Balaji MS, Raghavan S, Jha S (2011) Role of tactile and visual inputs in product evaluation: a multisensory perspective. Asia Pac J Mark Logist 23:513–530. https://doi.org/10.1108/13555851111165066

45. Spence C, Gallace A (2011) Multisensory design: reaching out to touch the consumer. Psychol Mark 28:267–308. https://doi.org/10.1002/mar.20392

46. Cool HEM (2000) The significance of snake jewellery hoards. Britannia 31:29. https://doi.org/10.2307/526917

47. Liang M, Wanli Z (2022) Emotional expression in jewellery design under the background of artificial intelligence. Expert Syst. https://doi.org/10.1111/exsy.13134

48. Bechtel HB (1978) Color and Pattern in Snakes (Reptilia, Serpentes). J Herpetol 12:521–532. https://doi.org/10.2307/1563357

49. Ramljak S (1997) Keeping Vigil: jewelry, touch and physical engagement. American Craft 57:38–41

50. Bekker T, Sturm J, Eggen B (2010) Designing playful interactions for social interaction and physical play. Pers Ubiquitous Comput 14:385–396. https://doi.org/10.1007/s00779-009-0264-1

51. Flacandji M, Krey N (2020) Remembering shopping experiences: the shopping experience memory scale. J Bus Res 107:279–289. https://doi.org/10.1016/j.jbusres.2018.10.039

52. Perrault ST, Lecolinet E, Eagan J, Guiard Y (2013) Watchit: simple gestures and eyes-free interaction for wristwatches and bracelets. In: Proceedings of the SIGCHI Conference on Human Factors in Computing Systems. ACM, New York, NY, pp 1451–1460. https://doi.org/10.1145/2470654.2466192

53. Hu DL, Nirody J, Scott T, Shelley MJ (2009) The mechanics of slithering locomotion. Proc Natl Acad Sci 106:10081. https://doi.org/10.1073/pnas.0812533106

54. Jayne BC (2020) What defines different modes of snake locomotion? Integr Comp Biol 60:156–170. https://doi.org/10.1093/icb/icaa017

55. Holthaus KB, Mlitz V, Strasser B, Tschachler E, Alibardi L, Eckhart L (2017) Identification and comparative analysis of the epidermal differentiation complex in snakes. Sci Rep 7:45338. https://doi.org/10.1038/srep45338

56. Dubansky BH, Close M (2019) A review of alligator and snake skin morphology and histotechnical preparations. J Histotechnol 42:31–51. https://doi.org/10.1080/01478885.2018.1517856

57. Sian Rutland C, Cigler P, Kubale V (2019) Reptilian skin and its special histological structures. Veterinary Anatomy and Physiology. IntechOpen. https://doi.org/10.5772/intechopen.84212

58. Tiner C, Bapat S, Nath SD, Atre SV, Malshe A (2019) Exploring convergence of snake-skin-inspired texture designs and additive manufacturing for mechanical traction. Procedia Manuf 34:640–646. https://doi.org/10.1016/j.promfg.2019.06.116

59. Toro A, Abdel-Aal HA, Zuluaga E, Cuervo P, Ballesteros LM, Sánchez JC, Rudas JS, Isaza C, Misiolek WZ (2021) Influence of surface morphology and internal structure on the mechanical properties and tribological response of boa red tail and python regius snake skin. J Mech Behav Biomed Mater 119:104497. https://doi.org/10.1016/j.jmbbm.2021.104497

60. Klein M-CG, Gorb SN (2012) Epidermis architecture and material properties of the skin of four snake species. J R Soc Interface 9:3140–3155. https://doi.org/10.1098/rsif.2012.0479

61. Lee JL, Thompson A, Mulcahy DG (2016) Relationships between numbers of vertebrae, scale counts, and body size, with implications for taxonomy in nightsnakes (Genus: *Hypsiglena*). J Herpetol 50:616–620. https://doi.org/10.1670/15-066

62. Young BA, Kardong KV (2010) The functional morphology of hooding in cobras. J Exp Biol 213:1521–1528. https://doi.org/10.1242/jeb.034447

63. Mori A, Jono T, Takeuchi H, Ding L, Silva A, Mahaulpatha D, Tang Y (2016) Morphology of the nucho-dorsal glands and related defensive displays in three species of Asian natricine snakes. J Zool 300:18–26. https://doi.org/10.1111/jzo.12357

64. Doucet SM, Meadows MG (2009) Iridescence: a functional perspective. J R Soc Interface 6:. https://doi.org/10.1098/rsif.2008.0395.focus

65. Ligon RA, McCartney KL (2016) Biochemical regulation of pigment motility in vertebrate chromatophores: a review of physiological color change mechanisms. Curr Zool 62:237–252. https://doi.org/10.1093/cz/zow051

66. Blösch-Paidosh A, Shea K (2019) Design heuristics for additive manufacturing validated through a user study. Journal of Mechanical Design 141:. https://doi.org/10.1115/1.4041051

67. Blakey-Milner B, Gradl P, Snedden G, Brooks M, Pitot J, Lopez E, Leary M, Berto F, du Plessis A (2021) Metal additive manufacturing in aerospace: a review. Mater Des 209:110008. https://doi.org/10.1016/j.matdes.2021.110008